LAWRENCE
LIVERMORE
NATIONAL
LABORATORY

UCRL-JRNL-214592

Long-Term Phase Instability in A Water-Quenched Uranium Alloy

L. L. Hsiung, J. Zhou

August 12, 2005

Journal of Materials Research

Long-Term Phase Instability in A Water-Quenched Uranium Alloy

L. M. Hsiung and J. Zhou

Lawrence Livermore National Laboratory
Chemistry and Materials Science Directorate
P.O. Box 808, L-352
Livermore, CA 94551-9900

Abstract

The U-6 wt.% Nb (U6Nb) alloy in water-quenched (WQ) state has been in service for a number of years. Its long-term reliability is affected by the changes of the alloy microstructure and mechanical properties during service. In this communication, the water quenched U-6 wt.% Nb (WQ-U6Nb) alloy in service for 15 years at ambient temperatures was studied using an analytical TEM analysis. We found that the long-term natural aging resulted in a disorder-order phase transformation, leading to the formation of anti-phase boundaries (APBs). The newly-found ordered phase was then identified by proposing two phase transform schemes, which were also discussed with regards to the potential subsequence of the microstructural evolution for the alloy in further service. The initial study also provides convincing evidence for the disorder-order transformation, which has been predicted by numerous studies to be a transient thermodynamic event before spinodal decomposition. This suggests that the long-term naturally aged WQ-U6Nb is a good model alloy to study thermodynamic and kinetic phenomena requiring chronic processes.

Uranium alloys have a variety of engineering applications that require a combination of high strength, good ductility and corrosion resistance [1-6]. The martensitic phase transformation and shape memory effects exhibited by U-Nb alloys have also gained increasing interests [7-9]. To obtain desired physical and mechanical properties, the alloys are generally subject to various heat treatments, including annealing, solution treatment, water quenching, and artificial aging at elevated temperatures [10-13]. Water quenching is one of the most important heat treatments. A water quenched U-6 wt.% Nb (WQ-U6Nb) from γ (bcc)-field solid solution has a microstructure containing martensitic phases that are supersaturated with Nb [6,12]. In the stresses-induced martensitic transformation, a variant of the low temperature α (orthorhombic) phase is usually formed. This phase is designated α' martensite since its lattice parameters differ from the equilibrium α phase. Two additional variant phases, a monoclinic distortion of α', named α'' martensite, or a tetragonal distortion of γ, named γ^o martensite, may also be formed within the water-quenched alloy. All these variant phases are Nb supersaturated. The uniformly distributed Nb in solid solution suppresses the diffusional decomposition reaction, resulting in improved mechanical properties (ductility and toughness) and excellent corrosion resistance [12-14].

These supersaturated, unstable phases are prone to decompose. Numerous studies have been carried out to investigate aging behavior of the alloy at different temperatures [12-14]. These studies provide important insights to understand the effects of aging at elevated temperatures on the mechanical properties. However, what is still missing is the aging behavior of the alloy at ambient temperatures. Since it is difficult to study natural aging (NA) of the alloy due largely to the sluggish kinetics involved, the aging mechanisms of WQ-U6Nb at ambient temperatures are not yet understood. WQ-U6Nb alloy has been in service for many years [10]. Recently, Anne and Hiromoto have measured the mechanical properties of WQ-U6Nb alloy in

service for 15 years. They found the yield strengths of the 15 years old alloy are greater than 196 MPa. Compared to the historical data (149 MPa) for the fresh water-quenched alloy, this is a 25% increment [15]. This study shows a significant strength increase for a WQ-U6Nb alloy in service for 15 years [15]. However, it is not known what causes this change, and what will be the subsequence of the change. These are in all the most important issues to be addressed regarding the reliability of the alloy in long-term service.

In present study, we investigate the phase instability in a WQ-U6Nb alloy that has been in service for 15 years. It is found that an ordering transformation has occurred, and a modeling framework indicates that the disorder-order transformation is the precursor of spinodal decomposition. The WQ-U6Nb alloy used for this investigation was wrought processed from Rocky Flats VAR ingot at the BWXT/Bechtel Y-12 plant. Detailed information regarding the fabrication process can be found in [6]. The naturally aged (NA) samples were obtained from a 15-year old alloy sample. Microstructures of the WQ and NA samples were examined using a JEOL 200CX transmission electron microscope (TEM). TEM foils were machined from the rod-shape samples and the finial thinning of the foils was prepared by twinjet electropolishing in a solution of 45 vol. % methanol, 45 vol. % butyl alcohol and 10 vol. % nitric acid at 50 V and –20°C.

Significant microstructural evolution over a long-term duration is observed. WQ-U6Nb alloy has a typical martensitic structure (Figure 1), in which a large volume fraction of twin domains is formed during rapid cooling process. This microstructure is consistent with other studies [10-13], as previously introduced. After 15 years in service, the martensitic structure remains. However, new microstructral features are observed as shown in Figure 2, in which the swirl-shape antiphase domain boundaries (APBs) can be readily seen using bright-field (Figure

2a) and dark-field (Figure 2b) TEM imaging technique. The contrast of antiphase domain boundary (also known as π boundary) is visible when the phase angle $\alpha = 2\pi\mathbf{g}\bullet\mathbf{P} = \pi$ and is invisible when $\alpha = 2\pi$ (where **g** is the reflection vector for imaging, and **P** is the displacement vector of APB) [16]. This can be used to verify antiphase domain boundaries. A typical **g•P** image-contrast analysis for APBs in a 15-year NA sample is shown in Figure 3. The bright field image in Figure 3a clearly displays the swirl-shape APBs. These APBs are visible in the dark field images that were obtained using $00\bar{1}$ (Figure 3b) and $0\bar{2}\bar{1}$ (Figure 3c) superlattice reflections. However, the APBs become invisible in Figure 3d which was obtained using a $0\bar{2}0$ fundamental reflection. These images in Figure 3 further confirmed that the swirl-shaped structures are APBs.

The APBs are generally formed as a result of a disorder-order transformation [17]. In essence, the ordered phase domain has the same crystal structure as that of the disordered phase domain, except that it takes up a superlattice arrangement because of the periodic occupation of lattice sites by specific atom species. Since no long-range diffusion is involved in this process, disorder-order transformation typically occurs at low temperatures, at which high thermal energy is not available [17]. In the following sections, two possible disorder-order transformation schemes are proposed to model the formation of new chemically ordered α″ phase in the naturally aged U6Nb alloy. Its structure is also identified by a comparison between observed and simulated diffraction patterns.

In the WQ-U6Nb alloy, the uranium to niobium atomic ratio is 86:14. After solution treatment and water quenching from high temperature γ phase, the 14% Nb atoms randomly distribute in the uranium matrix, forming a supersaturated, disordered solid solution. A niobium atom could occupy any lattice sites in the unit structure, as shown in Figure 4. To reduce free

energy of the system, Nb atoms tend to occupy specific positions in the unit structure to form order structure (Figure 4). For the ordering transformation of Scheme I, U atoms occupy the following three specific lattice sites of the ordered superlattice (4 lattice sites/unit cell): (0,5/6,1/2), (1/2,1/3,1/2), and (1/2,1/2,0), whereas the (0,0,0) lattice site is randomly occupied by U and Nb atoms, in which the probability of the site occupied by U and Nb are 44% and 56%, respectively. The systematic variations in the atomic positions result in different ordered-domains separated by APBs across which the atoms have the wrong immediate neighbors, which is illustrated in Figure 4a.

For the ordering transformation of Scheme II, U atoms occupy (0,5/6,1/2) and (1/2,1/3,1/2) lattice sites, whereas the (0,0,0) and (1/2,1/2,0) lattice sites are randomly occupied by U and Nb atoms, in which the probability of the sites occupied by U and Nb are 72% and 28%, respectively. This is shown in Figure 4b. Scheme II results in an ordered structure with alternative U-rich and Nb-rich layers. The wavelength of this structure is about 4.95 nm, which is close to the lattice parameter of α'' unit cell in the z-direction.

The [110]-, [310]-, [312]-, and [100]-zone selected-area diffraction (SAD) patterns generated from the 15-year NA sample are shown in Figures 5 and 6, in which the corresponding zone diffraction patterns simulated according to the Schemes I and II ordering transformations are also displayed. It is noted that the simulation patterns of the [110]- and [310]-zone are identical between Scheme I and II as shown in Figure 5, whereas the simulation patterns of the [001]-zone are different between Scheme I and II as shown in Figure 6. The ordering transformation of α'' phase is identified to be most likely of Scheme II type in accordance to the observed and simulated [100]-zone patterns as shown in Figure 6. The ordered structure resulting from schemed II has minimum elastic energy, but the greatest chemical gradient. This structure

may not be energy favored. The small wavelength (0.495 nm) is one order smaller than that of modulated structure resulting from spinodal decomposition at elevated temperatures [13,18]. The question is therefore what is the subsequence of this disorder-order transformation. If the ordering is the precursor of phase decomposition, how long will it take to accomplish the decomposition?

Fine-scale phase decomposition, namely spinodal decomposition, of the WQ-U6Nb has been experimentally studied at elevated temperatures [11,12,18] using microhardness testing. However, this method is not practical for natural aging, since a much longer duration is required to carry out such type of study. Hence, future kinetics studies may be employed to predict the microstructure evolution and the resulting mechanical property changes over longer time service in future. Nevertheless, this communication shows that the disorder-order transformation occurred within the WQ-U6Nb alloy at ambient temperatures over the past 15 years of service. This finding is critical and important in evaluating the mechanical performance and the reliability of this alloy in further service.

Before closing, it is worth noting that the naturally aged WQ-U6Nb alloy is important alloy system to study long-term phenomena in spinodal decomposition. A number of numerical studies have suggested that ordered transient phases should be formed before spinodal decomposition in several alloy systems, such as Au-Ni alloy [19, 20]. By heating a TEM foil made from the spinodally decomposed Au-Ni alloys, Zhao and Notis [21] observed reversely ordered transient phase at the edge of the TEM specimens [21]. It was, therefore, believed that the disorder-order transformation may be hindered by the elastic strain in a bulk alloy. However, such transient ordering has been never been directly confirmed by experimental observations, due largely to the difficulties associated with the kinetic process. The ordering process could be

too rapid to observe for some alloys [22, 23]. It could be so slow, taking years to observe the microstructure changes [18]. Our study, carried out on this WQ-U6Nb alloy after a service of 15 years, enables us to observe the disorder-order transform that is otherwise difficult to observe in other materials. In this sense, a 15-year naturally aged WQ-U6Nb alloy is a good model alloy to study phenomena associated with spinodal decomposition and other phase changes that require very long time to accomplish.

Acknowledgements

This work was performed under the auspices of the U. S. Department of Energy by the University of California, Lawrence Livermore National Laboratory under Contract No. W-7405-Eng-48. The authors gratefully acknowledge Bob McKoon, Anne Sunwoo, and T. C. Sun for their contribution to the heat treatment of the U6Nb alloy, Cheng Saw and Octavio Cervantes for the X-ray diffraction analysis, Bob Vallier and Vicki Mason-Reed for the microhardness measurement, and Rick Gross and Jessee Welch for the preparation of TEM foils.

References:

1. Bates LF and Barnard RD. Electrical and magnetic properties of uranium-niobium system. Proceedings of The Physical Society of London 1961; 78 (501): 361-68.
2. Suski W, Czopnik A, Solyga M, Wochowski K, Mydlarz T. Magnetic, electrical and thermodynamic properties of the UCu6Al6 derivatives. Physica B-Condensed Matter 2005; 359: 1024-1026.
3. Magness LS. High-strain rate deformation behavior of kinetic-energy penetrator materials during ballistic impact. Mechanics of Materials 1994; 17 (2-3): 147-154.
4. Nakamura K, Ogata T, Kurata M, Yokoo T and Mignanelli MA. Reactions of uranium-plutonium alloys with iron. Journal of Nuclear Science and Technology 2001; 38 (2): 112-119.
5. Kelly D, Lillard JA, Manner WL, Hanrahan R and Paffett MT. Surface characterization of oxidative corrosion of U-Nb alloys. Journal of Vaccum Science & Technology A-Vaccum Surfaces and Films 2001; 19 (4): 1959-1964.
6. Eckelmeyer KH, Romig AD and Weirick LJ. The effects of quench rate on the microstructure, mechanical properties, and corrosion behavior of U-6 WT PCT Nb. Metallurgical Transactions A- Physical Metallurgy and Materials Science 1984; 15 (7): 1319-1330.
7. Addessio FL, Zuo QH, Mason TA and Brinson LC. Model for high-strain-rate deformation of uranium-niobium alloys. Journal of Applied Physics 2003; 93 (12): 9644-9654.
8. Vandermeer RA, Ogle JC and Northcutt WG. A phenomenological study of the shape memory effect in polycrystal uranium niobium alloys. Metallurgical Transactions A-Physical Metallurgy and Materials Science 1981; 12 (5): 733-741.
9. Field RD, Brown DW and Thomas DJ. Texture development and deformation mechanisms during uniaxial straining of U-Nb shape-memory alloys. Philosophical Magazine 2005; 85 (13): 1441-1457.
10. Jackson RJ and Miley DV. Tensile properties of Gamma quenched and aged uramium-based niobium alloys. ASM Transactions 1968; 61 (2): 336-341
11. Orlov K, Teplinskaya VM, Chebotarev NT. Decomposition of a metastable solid solution in uranium-molybdenum alloy. Atomic Energy 2000; 88 (1): 42-47.

12. Vandermeer RA. Phase transformations in a uranium + 14 at. % niobium alloy. Acta Metallurgica. 1980; 28 (3): 383-393.
13. Beverini G, Edmonds DV. An APFIM study of the aging behavior of U-6 wt-percent Nb. Journal De Physique 1989; 50 (C8): C8429-C8434 Suppl. 11.
14. Koike J, Kassner ME, Tate RE and Rosen RS. The Nb-U (niobium-uranium) system Journal of Phase Equilibrium 1998; 19 (3): 253-260.
15. Sunwoo AJ and Hiromoto DS. Effects of natural aging on the tensile properties of water-quenched U-6%Nb alloy. Journal of Nuclear Materials 2004; 327 (1): 37-45.
16. Edington JW. Practical Electron Microscopy in Materials Science, Van Nostrand Reinhold, New York, 1976.
17. Easterling KE and Porter DA, Phase Transformation in Metals and Alloys, CRC Press, UK 1992.
18. Unpublished reports.
19. Cahn JW. Transaction of TMS and AIME 1968; 242 p. 166.
20. Mbaye AA, Ferreira LG and Zunger A. 1st-principles calculation of semiconductor-alloy phase diagrams, Physical Review Letters 1987; 58 (1): 49-52.
21. Zhao JC and Notis MR. Ordering transformation and spinodal decomposition in Au-Ni alloys. Metallurgical and Materials Transactions 1999; 30A: 707-716.
22. Sato K and Stobbs WM. Quantification of the spinodal wave in Cu2.5Mn0.5Al by dark-field image analysis. Philosophic Magazine A-Physics of Condensed Matter Structure Deffects and Mechanical Properties 1994; 69 (2): 349-377.
23. Butler EP and THOMAS G. Structure and properties of spinodally decomposed Cu-Ni-Fe alloys. Acta Metallurgica 1970; 18 (3): 347& 1970.

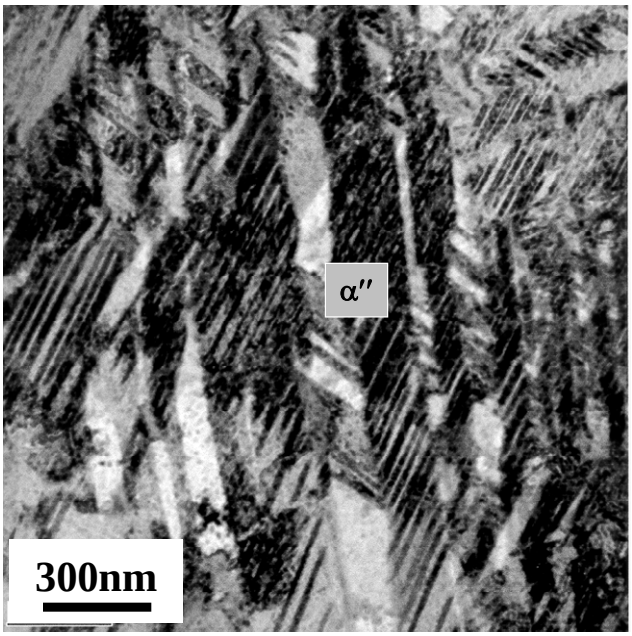

Figure 1: Martensitic microstructure in the WQ U6Nb alloy.

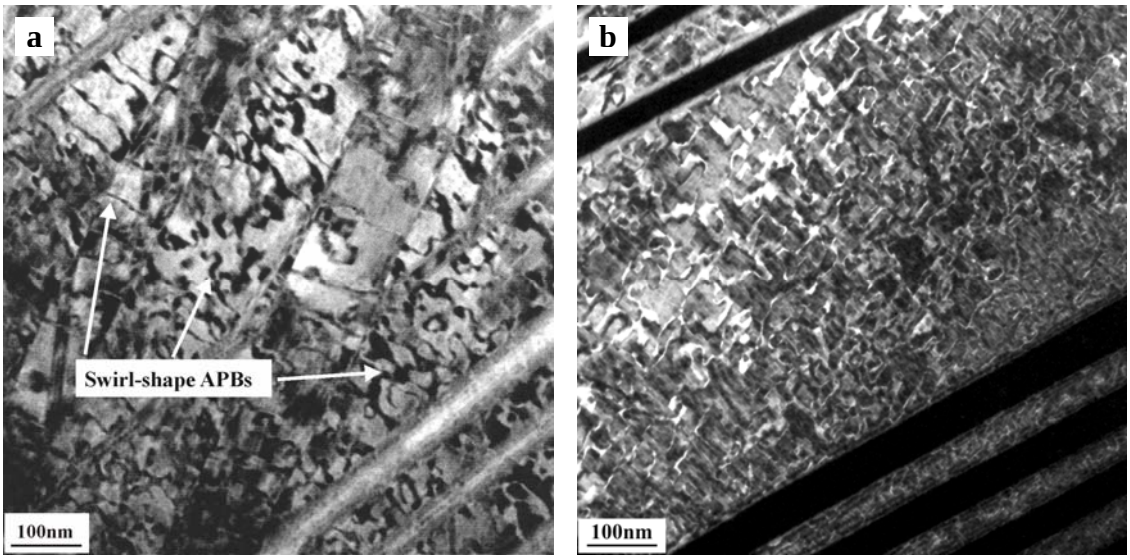

Figure 2: Bright-field (a) and dark-field (b) TEM images reveal the formation of swirl-shape antiphase domain boundaries (APBs) within the 15-year NA sample. Notice that APBs appear as a dark contract in (a) and a bright contrast in (b).

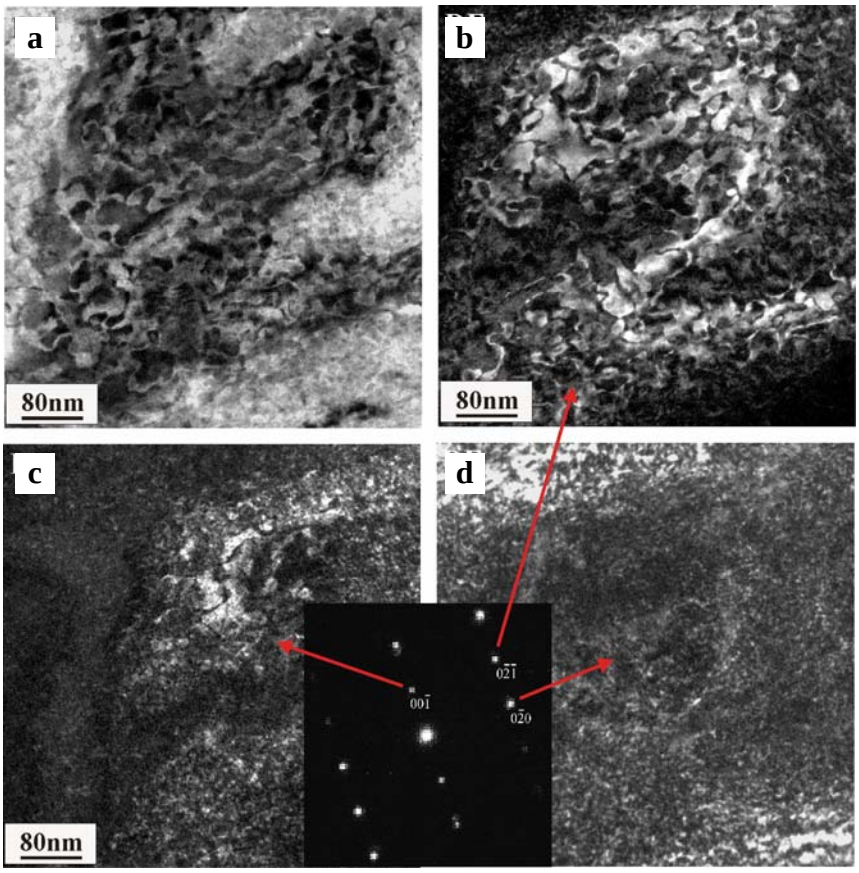

Figure 3: BF and DF images of growth APBs in an ordered α″ domain observed in the same area. The APBs are visible using $00\bar{1}$ and $0\bar{2}\,\bar{1}$ superlattice reflections but become invisible when using $0\bar{2}\,0$ fundamental reflection to image.

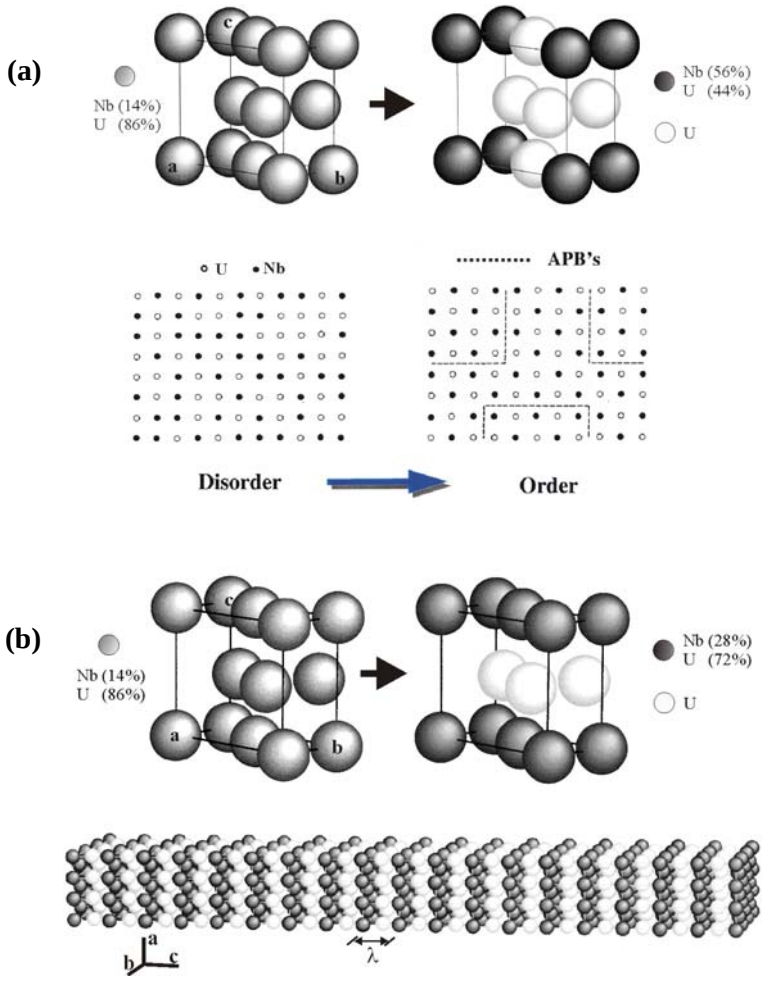

Figure 4: Schematic illustrations showing two possible schemes proposed for the disorder-order transformation occurred in the binary U-14at%Nb (U-6wt%Nb) alloy, in which two different partially ordered α″ unit cells can be generated according to (a) Scheme I. and (b) Scheme II ordering transformation.

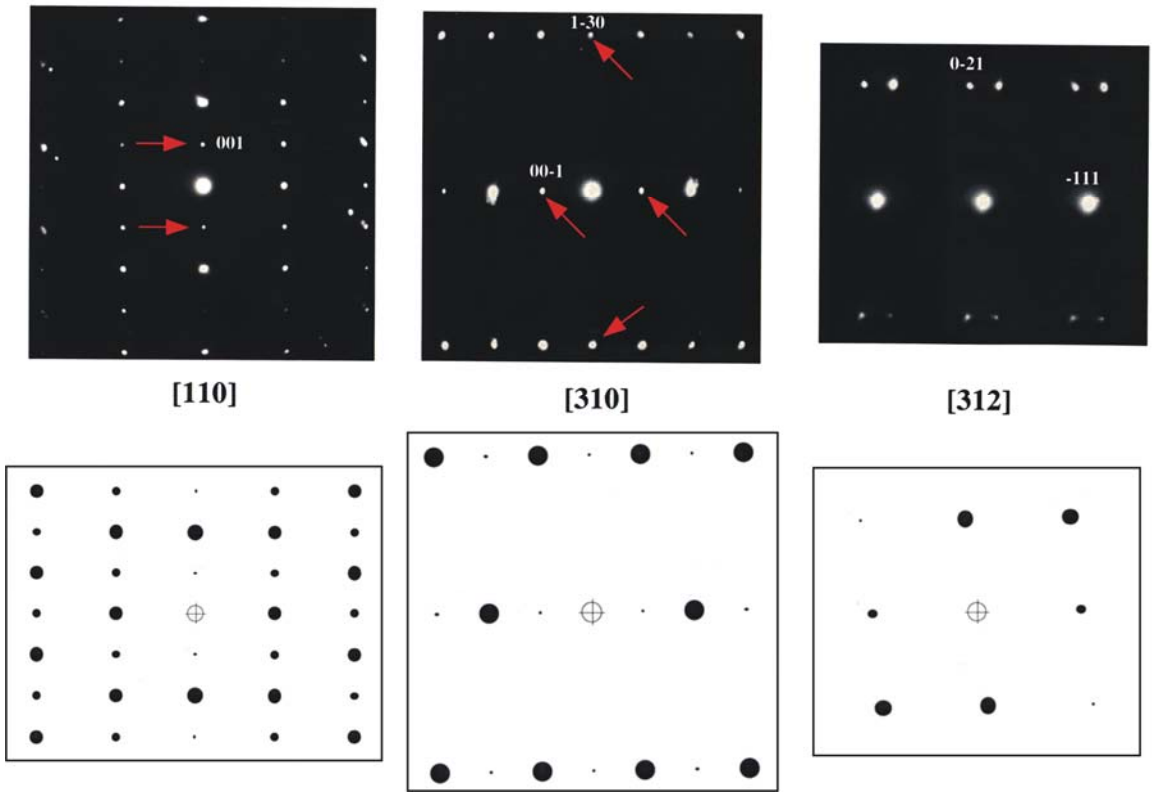

Figure 5: The [110]-, [310]-, and [312]-zone diffraction patterns generated from the 15-year NA sample, in which the superlattice spots are arrowed (upper). The corresponding zone diffraction patterns simulated for the proposed ordered α″ unit cell according to Schemes I and II ordering transformation are shown below.

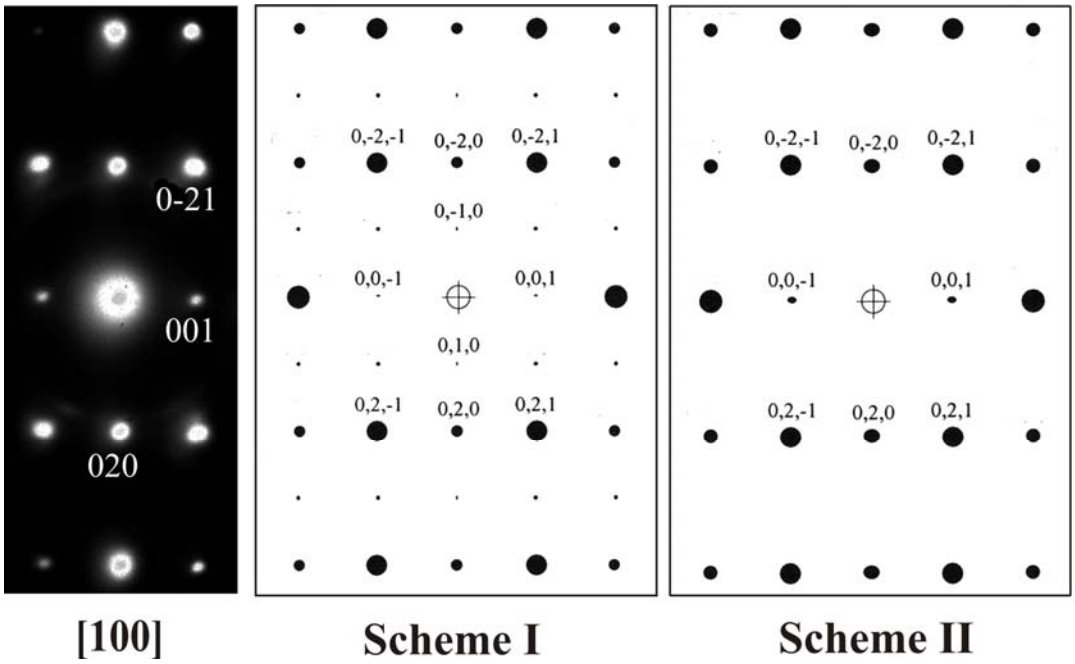

Figure 6: The [100]-zone diffraction pattern generated from 15-yr NA sample shown with simulated patterns based upon scheme I and scheme II unit cells. Here, scheme II is more likely to be the one for the partially ordered α″ phase according to the comparison between observed and simulated patterns.